Electronic Supplementary Material (ESI) for Faraday Discussions.
This journal is © The Royal Society of Chemistry 2023

Designing Mixed-Metal Electrocatalyst Systems for Photoelectrochemical Dinitrogen Activation

Manpreet Kaur, Marc Walker, Steven Hindmarsh, Charlotte Bolt, Stephen York, Yisong Han, Martin R. Lees, Katharina Brinkert*

*katharina.brinkert@warwick.ac.uk

Contents

1 Nitrogen 1s XP spectra

Sample XP spectra for the N 1s region were obtained for consecutively deposited p-InP-Mo-Co electrodes from the Na_2MoO_4 and $CoCl_2$-based electrolytes and p-InP-CoMo electrodes prepared by co-photoelectrodeposition in the presence of boric acid. Both spectra do not indicate the presence of nitrogen on the photoelectrode surface.

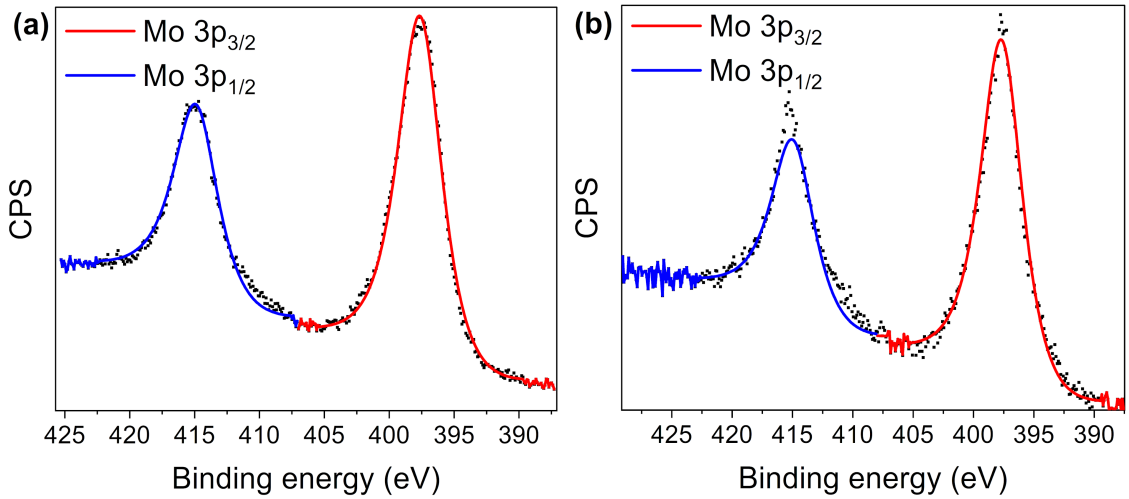

Fig. S1 XP spectra of **(a)** consecutively deposited p-InP-Mo-Co photoelectrodes from Na_2MoO_4 and $CoCl_2$ electrolytes, and **(b)** a p-InP-CoMo photoelectrode prepared by co-deposition in the presence of boric acid. Shown is the Mo 3p and N 1s region.

2 Grain masks used in Gwyddion to calculate maximum height distributions

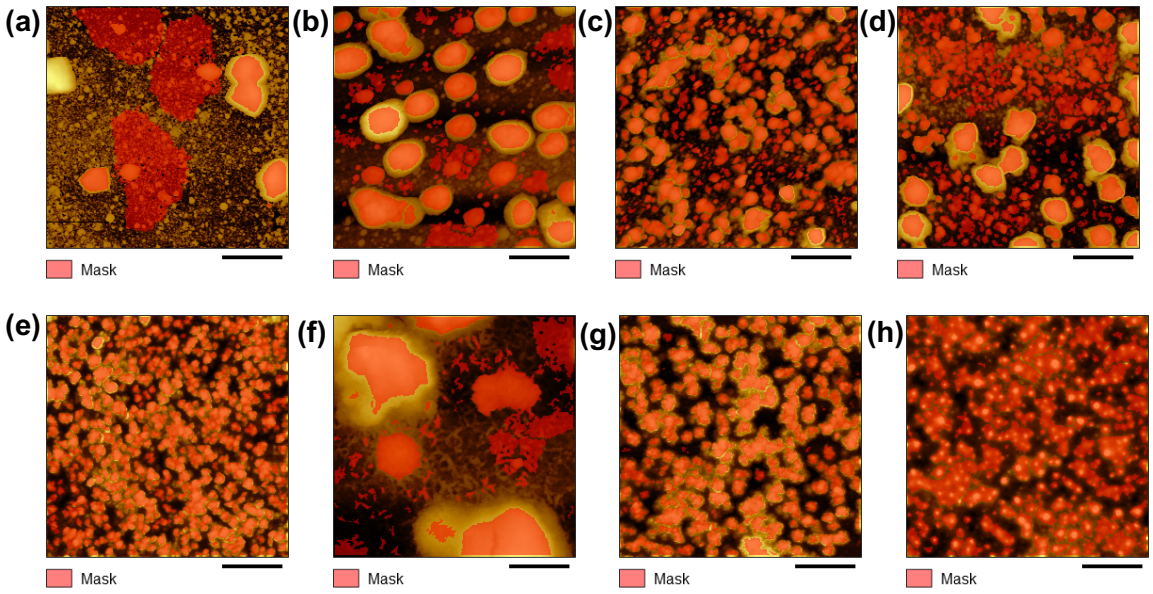

Fig. S2 AFM images (scale bar 500 nm) masked using the watershed method to calculate the maximum height distribution data of the grains. **(a)** is the Na_2MoO_4 - $CoCl_2$ deposition, **(b)** is the Na_2MoO_4 - $CoSO_4$ deposition, **(c)** is the $MoCl_3$ - $CoSO_4$ deposition, **(d)** is the $MoCl_3$ - $CoCl_2$ deposition, **(e)** is the CoMo co-deposition with boric acid, **(f)** is CoMo co-deposition without boric acid, **(g)** is CoMo-Ru consecutive deposition and **(h)** is the CoMoRu co-deposition.

3 Table of XPS binding energies

Table S1. XPS binding energies obtained for the Mo $3d_{5/2}$ region and component 1 of the Co $2p_{3/2}$ region.[1,2]

Species	**Oxidation state**	**Binding energies (eV)**
Mo $3d_{5/2}$	Mo^0	227.7 - 229.1
	Mo^{2+}	229.4
	Mo^{4+}	230.5 - 232.0
	Mo^{6+}	231.8 - 232.8
Co $2p_{3/2}$	Co^0	777.5 - 777.9
	Co^{2+}	780.9 - 781.3
Mo $3p_{3/2}$	Mo^{6+} (Mo-N)	397.8
N 1s	Mo-N	398.1
	$Mo\text{-}NH_2$	400.3
	$Mo\text{-}NH_3^+$	402.5

4 Magnetisation of the p-InP substrate

The magnetisation *vs* applied field plots at 5 K and 300 K for the p-InP substrate (**Fig. S13 (a)**) were fitted with a simple linear field response and used to estimate the diamagnetic contribution in the magnetisation data that arises from the substrate of each film. The magnetic susceptibility, M/H, of approximately -300 × 10^{-9} emu/g is in reasonable agreement with previous reports.[3]

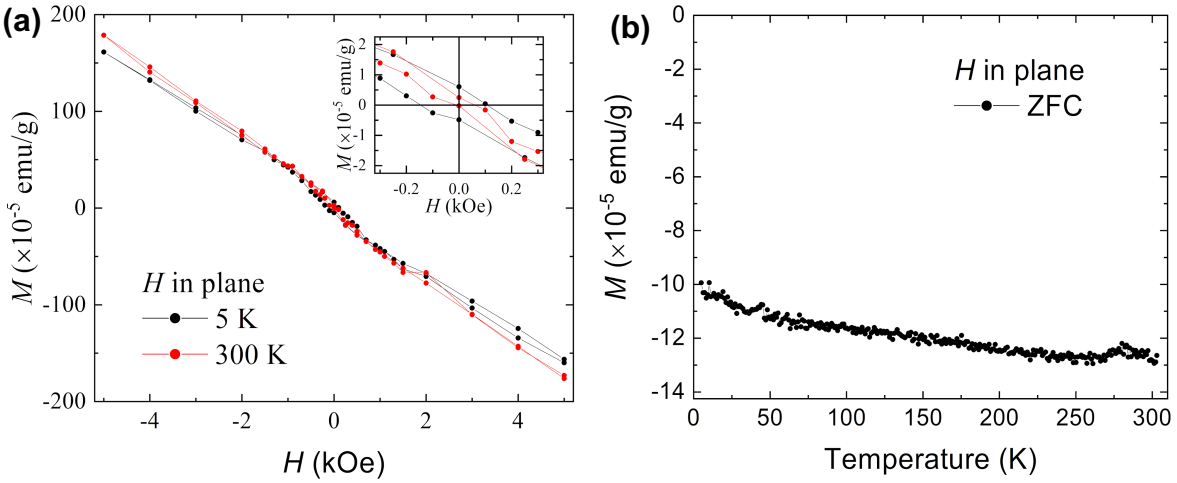

Fig. S3 Magnetisation *vs* applied field plots at 5 K and 300 K of p-InP **(a)** and magnetisation *vs* temperature data collected in a magnetic field of 250 Oe with the field applied in the plane of the p-InP substrate **(b)**.

5 XP spectrum of $MoCl_3$ reagent

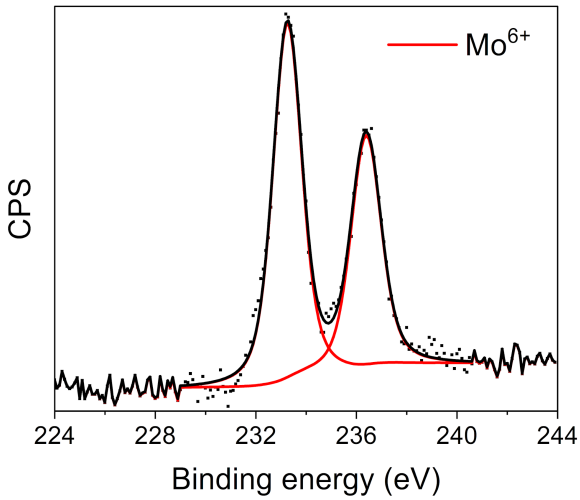

Fig. S4 XP spectrum of the Mo 3d component in the $MoCl_3$ reagent.

6 Photoelectrode surface characterisation

6.1 Consecutive photoelectrodeposition from Na_2MoO_4 - $CoCl_2$ electrolytes

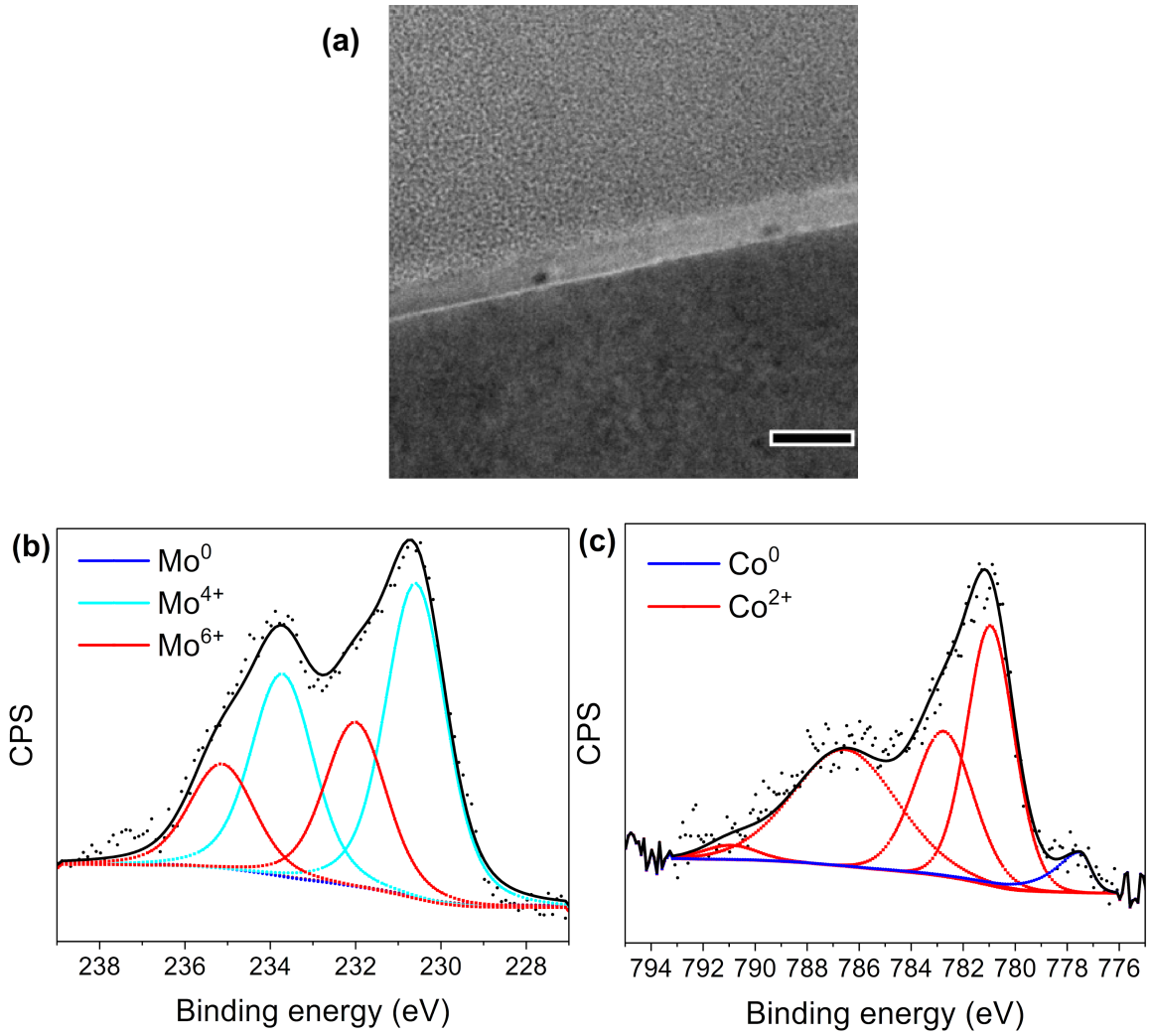

Fig. S5 Cross-sectional TEM image with a 50 nm scale bar **(a)**, XP spectrum of Mo 3d **(b)**, and XP spectrum of Co $2p_{3/2}$ **(c)** for the p-InP-Mo-Co electrodes prepared via photoelectrodeposition. Mo deposition was realised from an aqueous solution of Na_2MoO_4 (10 mM), Na_2SO_4 (1 M), and H_3BO_3 (0.5 M) at a potential of -0.09 V *vs* RHE applied for 10 s. Subsequent Co deposition occurred from an aqueous solution of $CoCl_2$ (0.1 M), NaCl (0.5 M) and 2-propanol (0.5% v/v) at a potential of -0.09 V *vs* RHE applied for 3 s. An Xe arc lamp with a power density of 100 mW/cm^2 was used as an illumination source.

6.2 Consecutive photoelectrodeposition from Na_2MoO_4 - $CoSO_4$ electrolytes

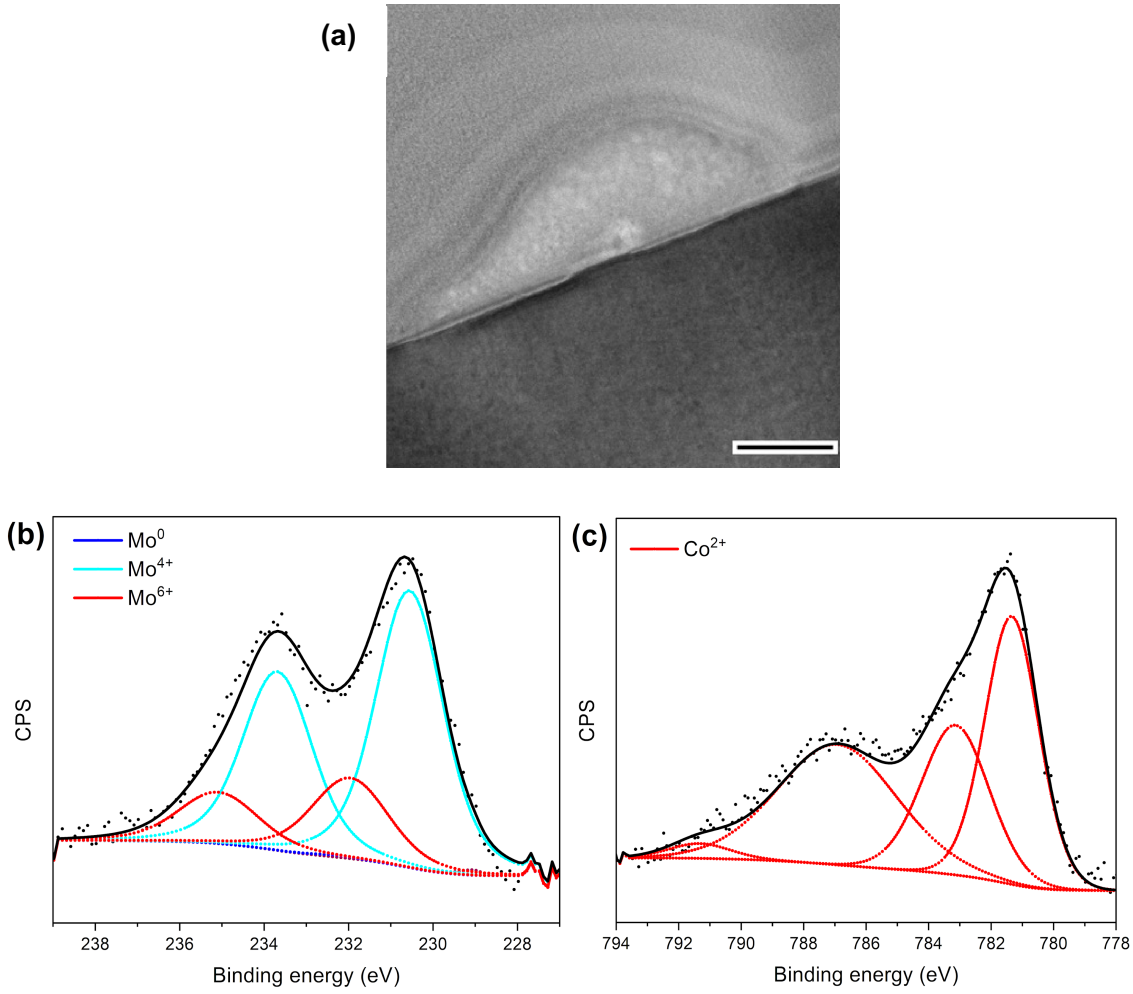

Fig. S6 Cross-sectional TEM image with a 150 nm scale bar **(a)**, XP spectrum of Mo 3d **(b)**, and XP spectrum of Co $2p_{3/2}$ **(c)** for the p-InP-Mo-Co electrodes prepared via photoelectrodeposition. Mo deposition was realised from an aqueous solution of Na_2MoO_4 (10 mM), Na_2SO_4 (1 M), and H_3BO_3 (0.5 M) at a potential of -0.09 V *vs* RHE applied for 10 s. Subsequent Co deposition occurred from an aqueous solution of $CoSO_4$ (0.2 M), Na_2SO_4 (1 M), and H_3BO_3 (0.5 M) at a potential of -0.09 V *vs* RHE applied for 3 s. An Xe arc lamp with a power density of 100 mW/cm^2 was used as an illumination source.

6.3 Consecutive photoelectrodepositions from $MoCl_3$ - $CoSO_4$ electrolytes

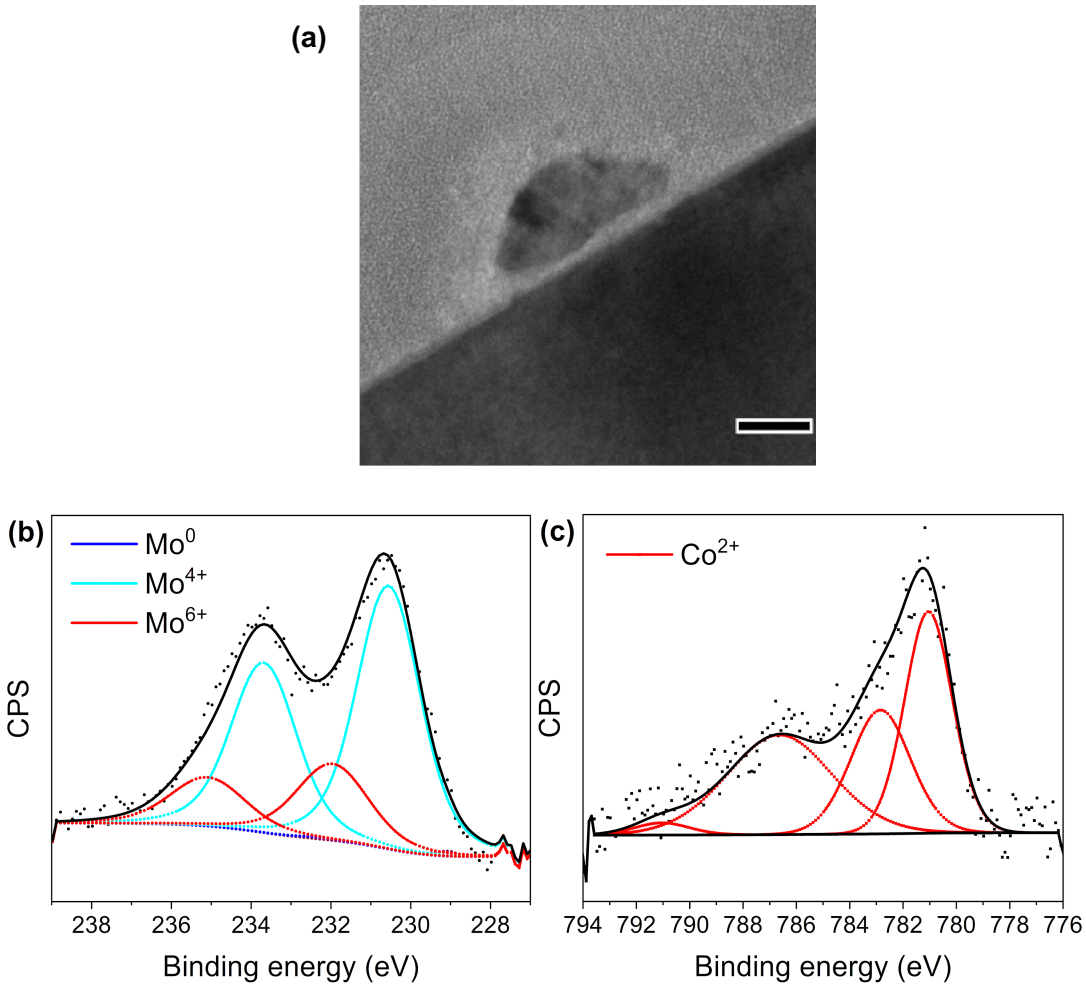

Fig. S7 Cross-sectional TEM image with a 50 nm scale bar **(a)**, XP spectrum of Mo 3d **(b)**, and XP spectrum of Co $2p_{3/2}$ **(c)** for the p-InP-Mo-Co electrodes prepared via photoelectrodeposition. Mo deposition was realised from an aqueous solution of $MoCl_3$ (1 mM), NaCl (0.5 M) and 2-propanol (0.5% v/v) at a potential of -0.09 V *vs* RHE applied for 10 s. Subsequent Co deposition occurred from an aqueous solution of $CoSO_4$ (0.2 M), Na_2SO_4 (1 M), and H_3BO_3 (0.5 M) at a potential of -0.09 V *vs* RHE applied for 3 s. An Xe arc lamp with a power density of 100 mW/cm^2 was used as an illumination source.

6.4 Consecutive photoelectrodepositions from $MoCl_3$ - $CoCl_2$ electrolytes

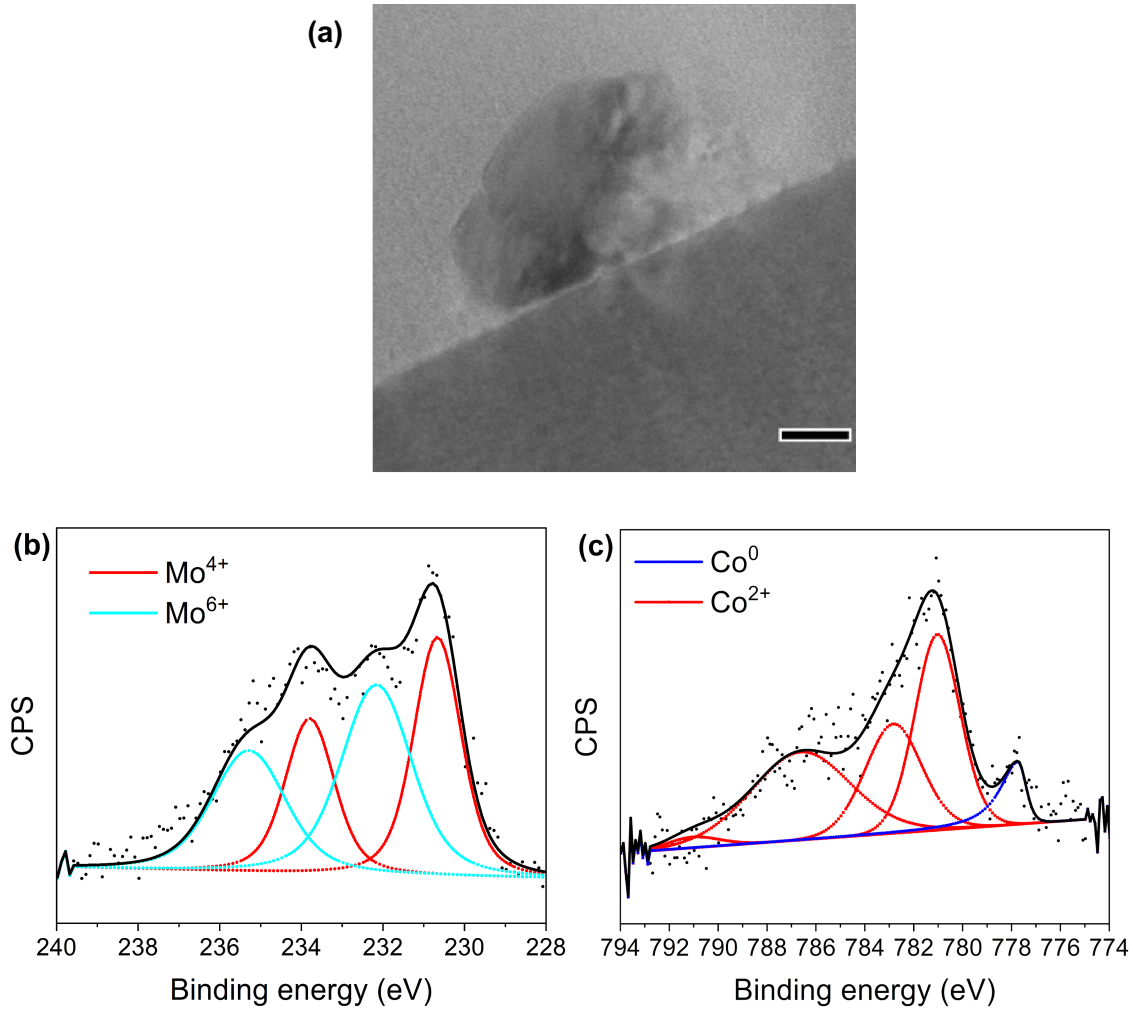

Fig. S8 Cross-sectional TEM image with a 50 nm scale bar **(a)**, XP spectrum of Mo 3d **(b)**, and XP spectrum of Co $2p_{3/2}$ **(c)** for the p-InP-Mo-Co electrodes prepared via photoelectrodeposition. Mo deposition was realised from an aqueous solution of $MoCl_3$ (1 mM), NaCl (0.5 M) and 2-propanol (0.5% v/v) at a potential of -0.09 V *vs* RHE applied for 10 s. Subsequent Co deposition occurred from an aqueous solution of $CoCl_2$ (0.1 M), NaCl (0.5 M) and 2-propanol (0.5% v/v) at a potential of -0.09 V *vs* RHE applied for 3 s. An Xe arc lamp with a power density of 100 mW/cm^2 was used as an illumination source.

6.5 Co-photoelectrodeposition of CoMo in the presence of boric acid

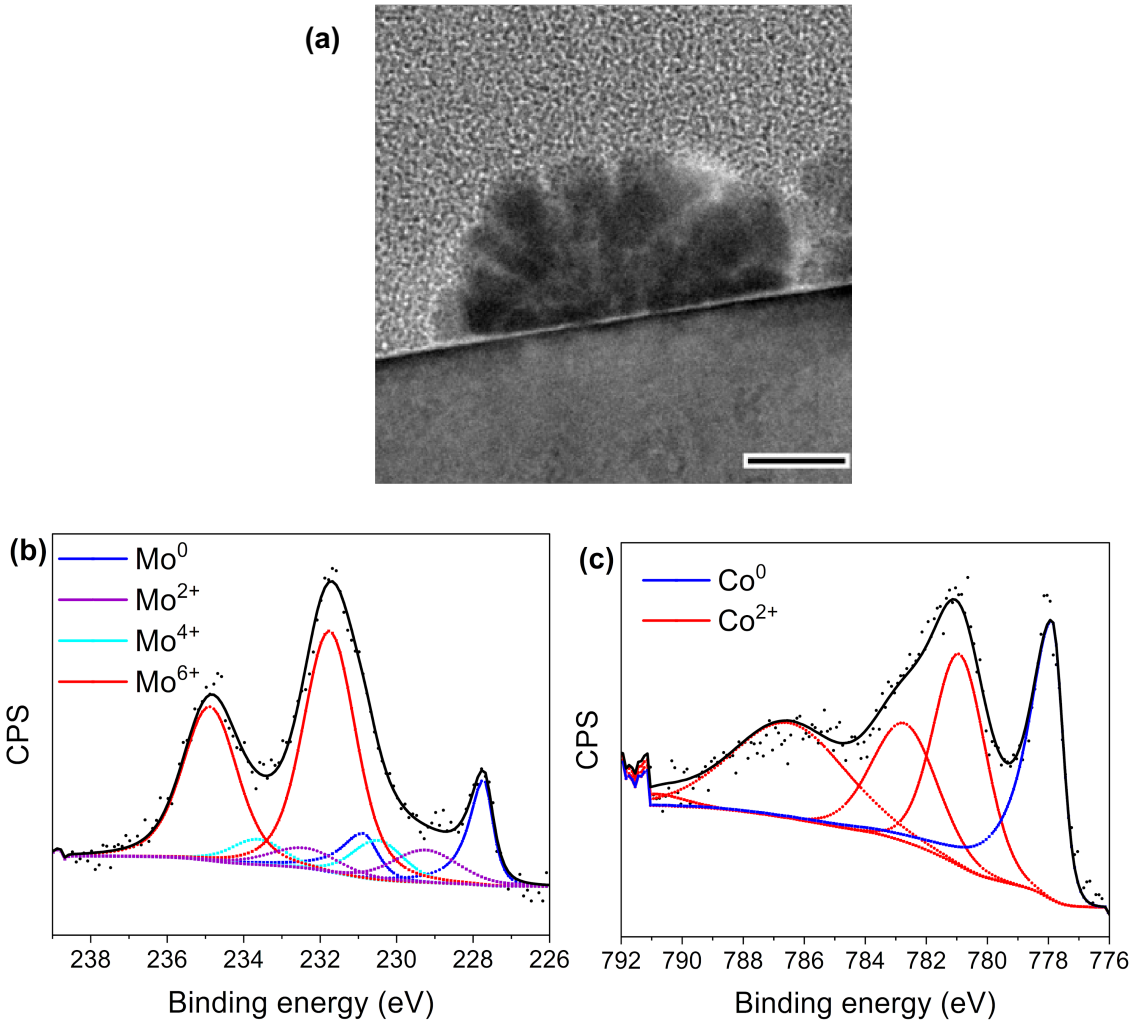

Fig. S9 Cross-sectional TEM image with a 40 nm scale bar **(a)**, XP spectrum of Mo 3d **(b)**, and XP spectrum of Co $2p_{3/2}$ **(c)** for the p-InP-CoMo electrodes prepared via co-photoelectrodeposition. An aqueous solution of $CoSO_4$ (0.2 M), Na_2MoO_4 (10 mM), Na_2SO_4 (1 M), and H_3BO_3 (0.5 M) was used for the deposition and a potential of -0.09 V *vs* RHE was applied for 10 s. An Xe arc lamp with a power density of 100 mW/cm^2 was used as an illumination source.

6.6 Co-photoelectrodeposition of CoMo in the absence of boric acid

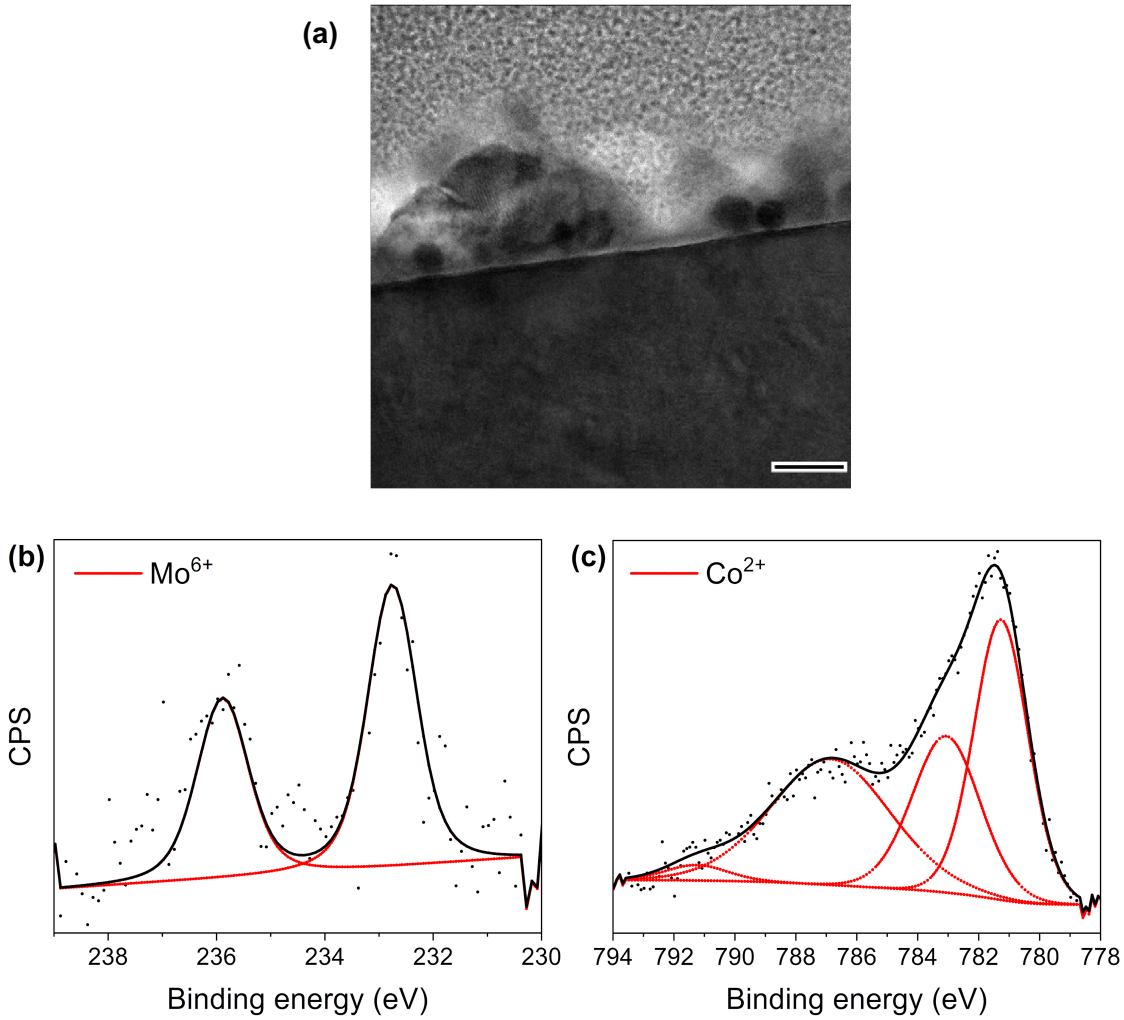

Fig. S10 Cross-sectional TEM image with a 20 nm scale bar **(a)**, XP spectrum of Mo 3d **(b)**, and XP spectrum of Co $2p_{3/2}$ **(c)** for the p-InP-CoMo electrodes prepared via co-photoelectrodeposition. An aqueous solution of $CoSO_4$ (0.2 M), Na_2MoO_4 (10 mM), and Na_2SO_4 (1 M) was used for the deposition and a potential of -0.09 V *vs* RHE was applied for 10 s. An Xe arc lamp with a power density of 100 mW/cm^2 was used as an illumination source.

7 Co-photoelectrodepositions of Co, Mo and Ru

7.1 p-InP-CoMo-Ru photoelectrodes

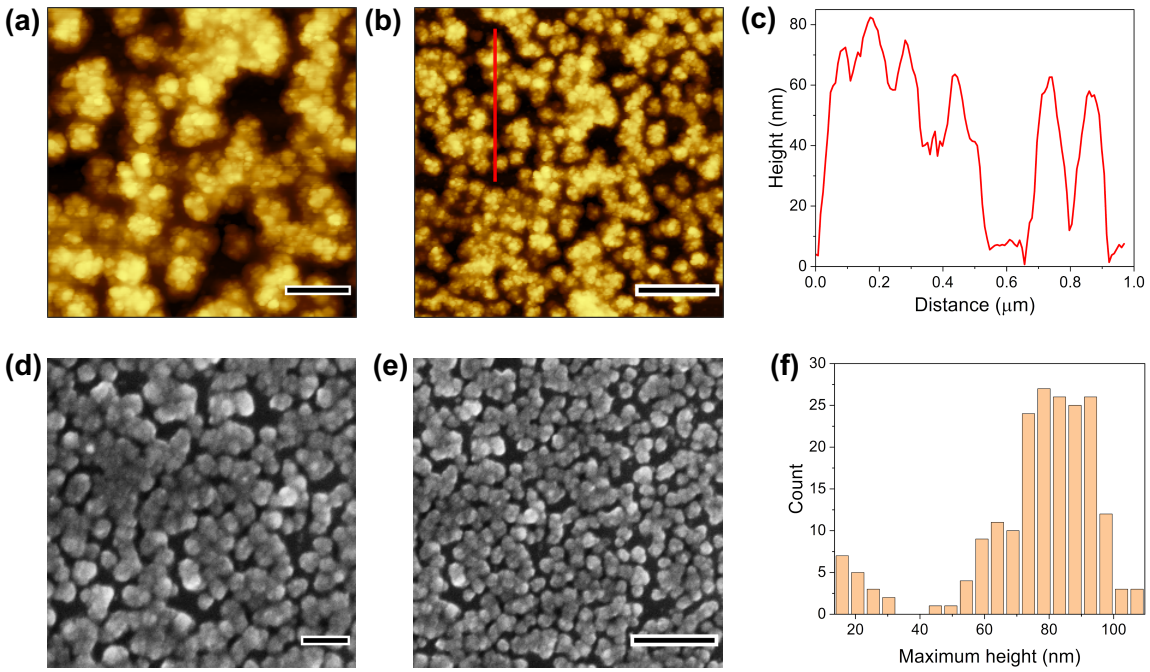

Fig. S11 Optical analyses of the p-InP-CoMo-Ru photoelectrodes. AFM images of the electrode surface are shown with a scale bar of 200 nm **(a)** and 500 nm **(b)** with a corresponding particle height analysis **(c)** across 980 nm of the electrode surface. **(d)** and **(e)** show SEM images of the surface with scale bars of 200 nm and 500 nm, respectively. **(f)** provides an overview of the maximum particle heights found on the electrode surface. CoMo deposits were obtained firstly via photoelectrodeposition from an aqueous solution of $CoSO_4$ (0.2 M), Na_2MoO_4 (10 mM), Na_2SO_4 (1 M), and H_3BO_3 (0.5 M) at a potential of -0.09 V *vs* RHE applied for 10 s. Subsequent Ru deposition occurred from an aqueous solution of $RuCl_3$ (0.33 mM), NaCl (0.5 M) and 2-propanol (0.5% v/v) at a potential of -0.09 V *vs* RHE applied for 5 s. An Xe arc lamp with a power density of 100 mW/cm^2 was used as an illumination source.

7.2 p-InP-CoMoRu photoelectrodes

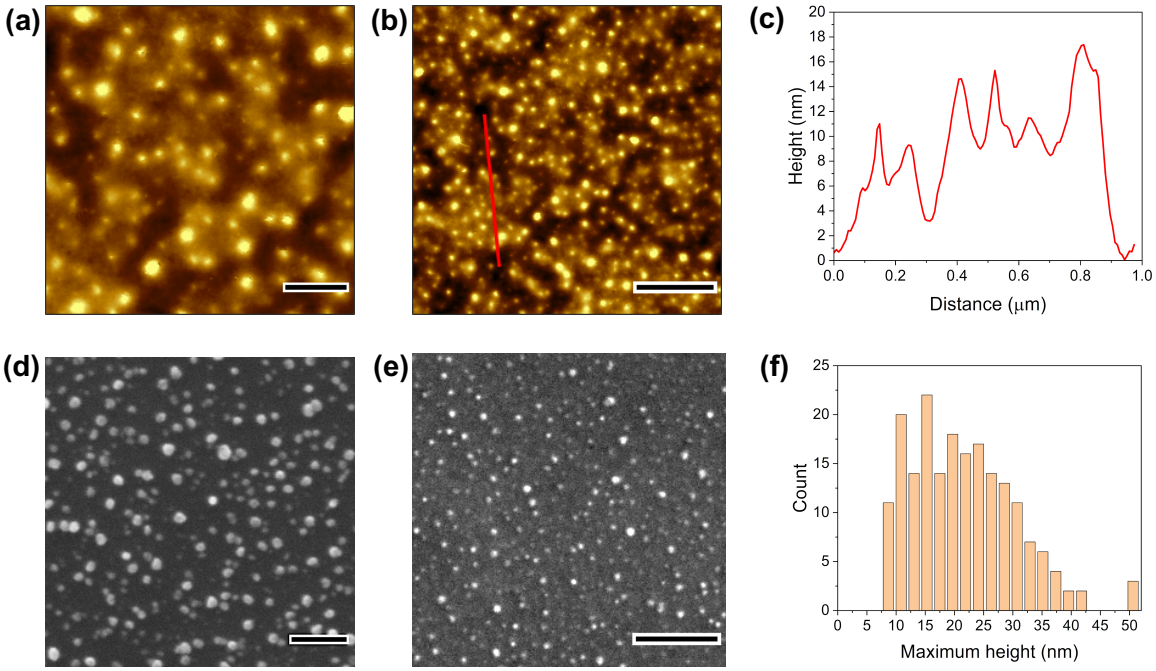

Fig. S12 Optical analysis of the p-InP-CoMoRu photoelectrodes. CoMoRu deposits were obtained from co-photoelectrodeposition from an aqueous solution of $CoCl_2$ (2 mM), $MoCl_3$ (0.1 mM), $RuCl_3$ (0.1 mM), H_3BO_3 (0.1 M), and NaCl (0.5 M) at a potential of -0.09 V *vs* RHE applied for 5 s. AFM images of the electrode surface are shown with a scale bar of 200 nm **(a)** and 500 nm **(b)** with a corresponding particle height analysis **(c)** across 980 nm. **(d)** and **(e)** show SEM images of the surface with scale bars of 200 nm and 500 nm, respectively. **(f)** provides an overview of the maximum particle height distribution found on the electrode surface.

8 Magnetometry data for the consecutively deposited electrodes

8.1 Consecutive photoelectrodepositions from Na_2MoO_4-$CoCl_2$ electrolytes

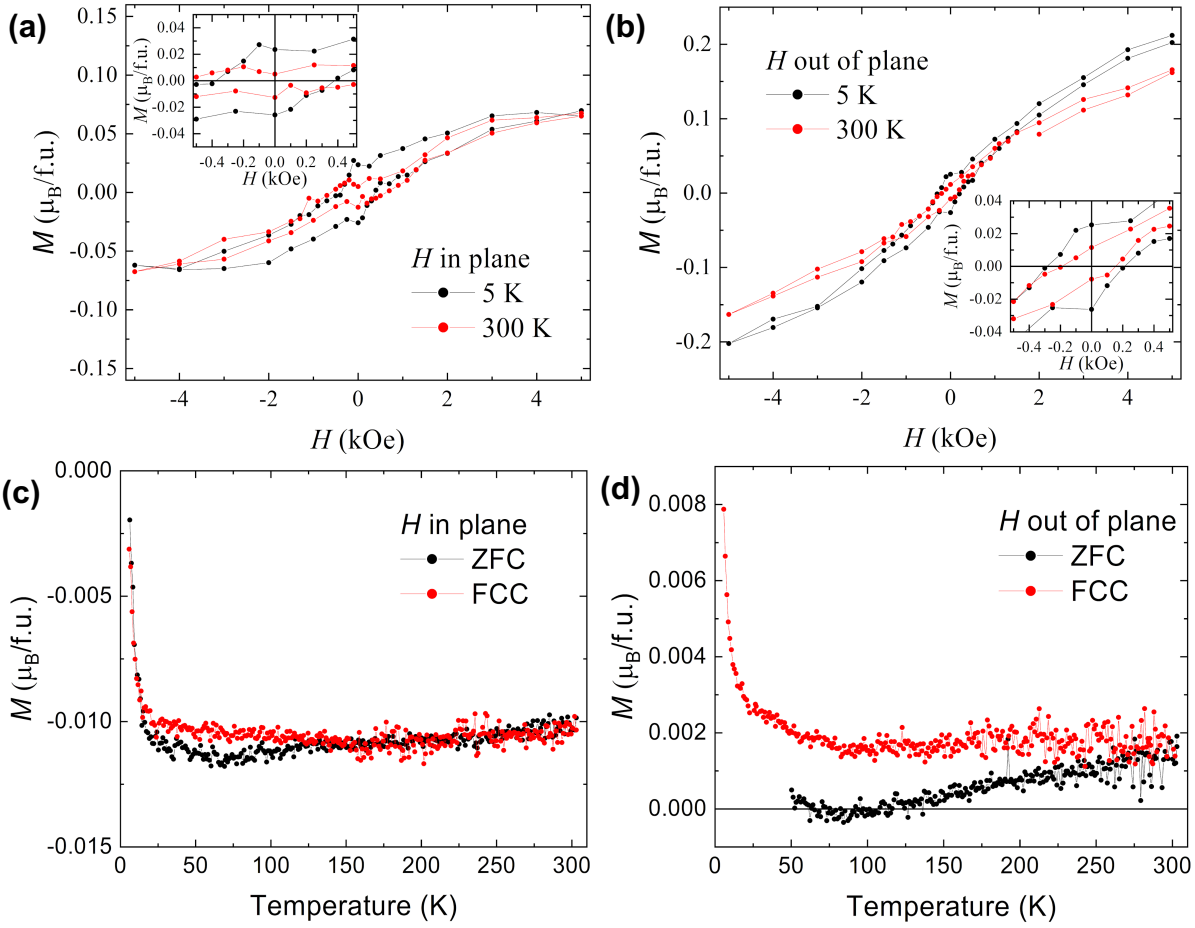

Fig. S13 Magnetisation *vs* applied field plots at 5 K and 300 K with a magnetic field applied in plane **(a)** and out of plane **(b)** of the deposited film. Magnetisation vs temperature data collected in a magnetic field of 250 Oe with the field applied either parallel **(c)** or perpendicular to the plane **(d)** of the deposited film for photoelectrodepositions using Na_2MoO_4 and $CoCl_2$ electrolytes.

8.2 Consecutive photoelectrodepositions from Na_2MoO_4 - $CoSO_4$ electrolytes

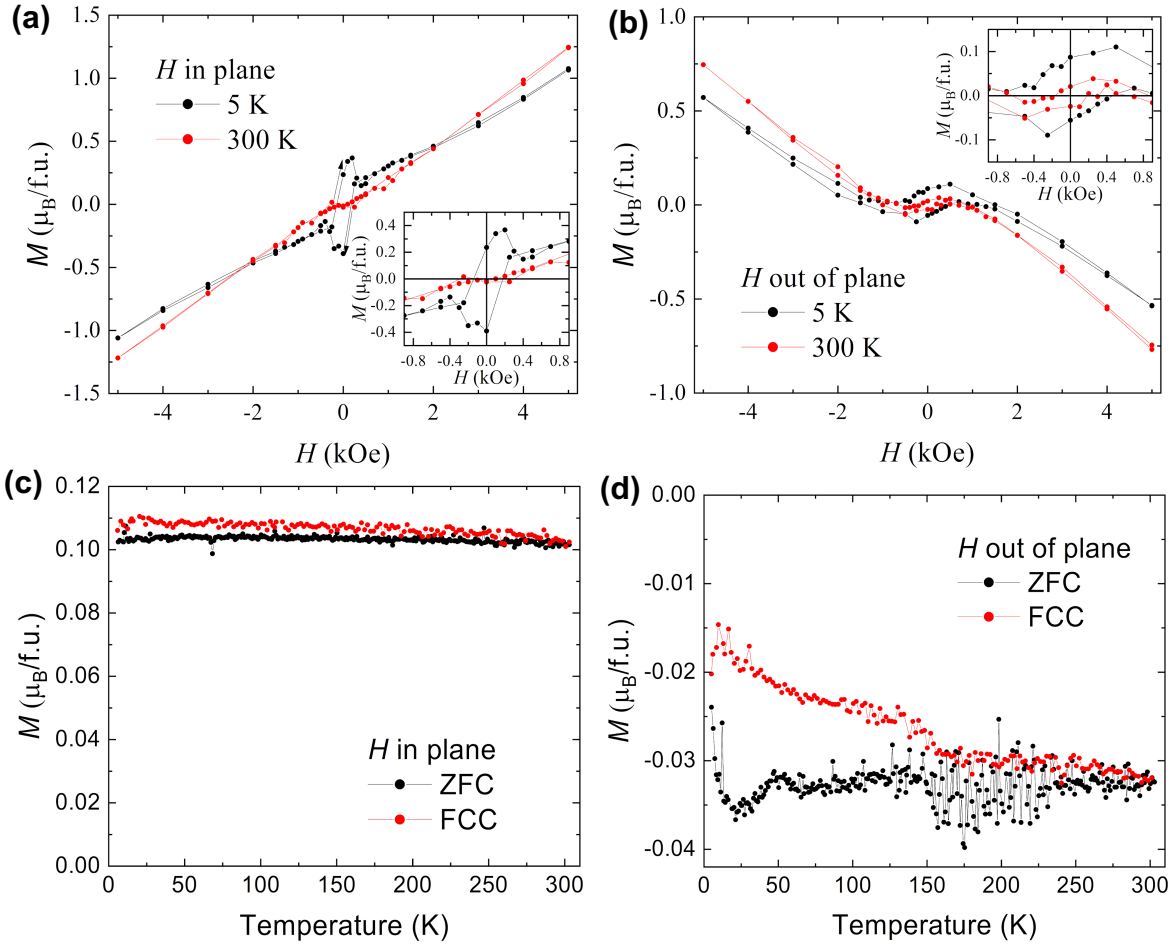

Fig. S14 Magnetisation *vs* applied field plots at 5 K and 300 K with a magnetic field applied in plane **(a)** and out of plane **(b)** of the deposited film. Magnetisation vs temperature data collected in a magnetic field of 250 Oe with the field applied either parallel **(c)** or perpendicular to the plane **(d)** of the deposited film for photoelectrodepositions using Na_2MoO_4 and $CoSO_4$ electrolytes.

8.3 Consecutive photoelectrodepositions from $MoCl_3$ - $CoSO_4$ electrolytes

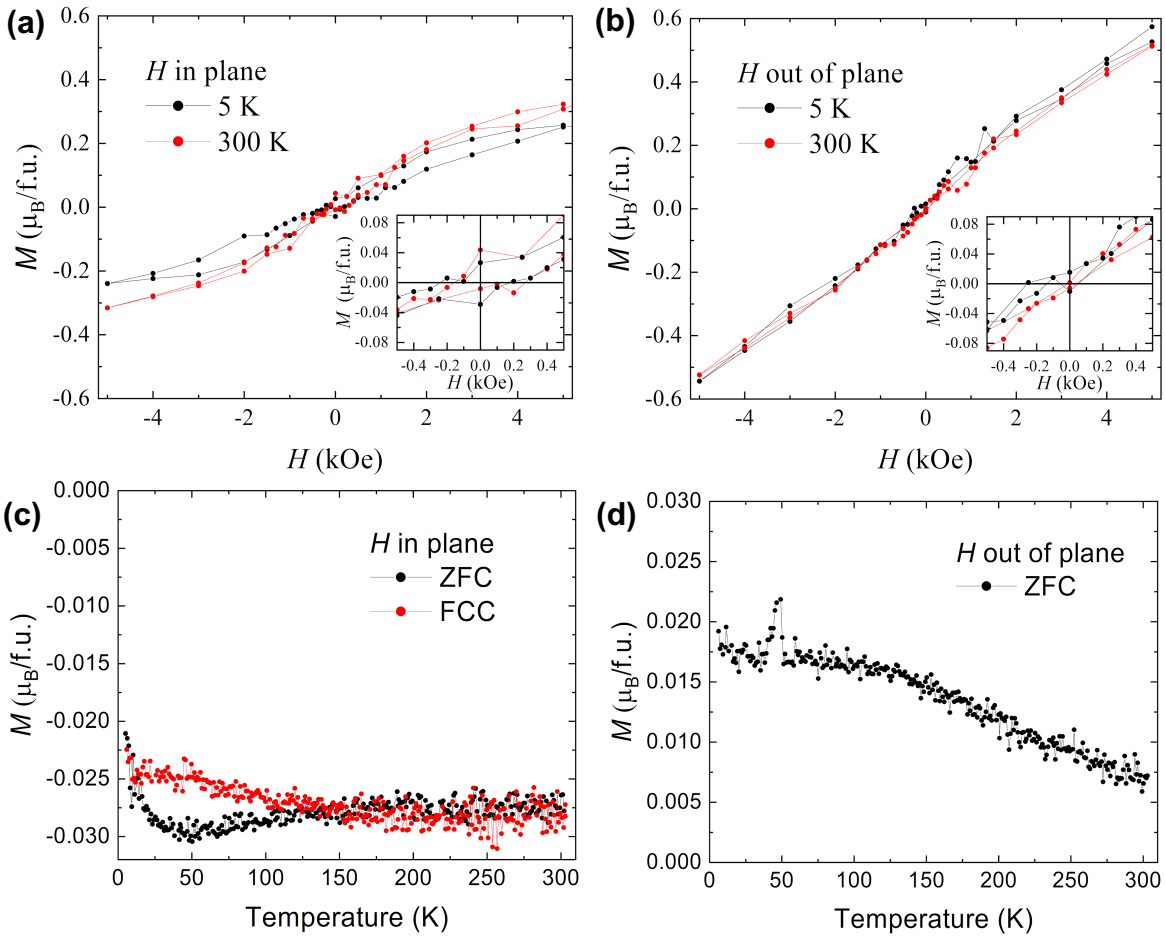

Fig. S15 Magnetisation *vs* applied field plots at 5 K and 300 K with a magnetic field applied in plane **(a)** and out of plane **(b)** of the deposited film. Magnetisation *vs* temperature data collected in a magnetic field of 250 Oe with the field applied either parallel **(c)** or perpendicular to the plane **(d)** of the deposited film for photoelectrodepositions using $MoCl_3$ and $CoSO_4$ electrolytes.

8.4 Consecutive photoelectrodepositions from $MoCl_3$ - $CoCl_2$ electrolytes

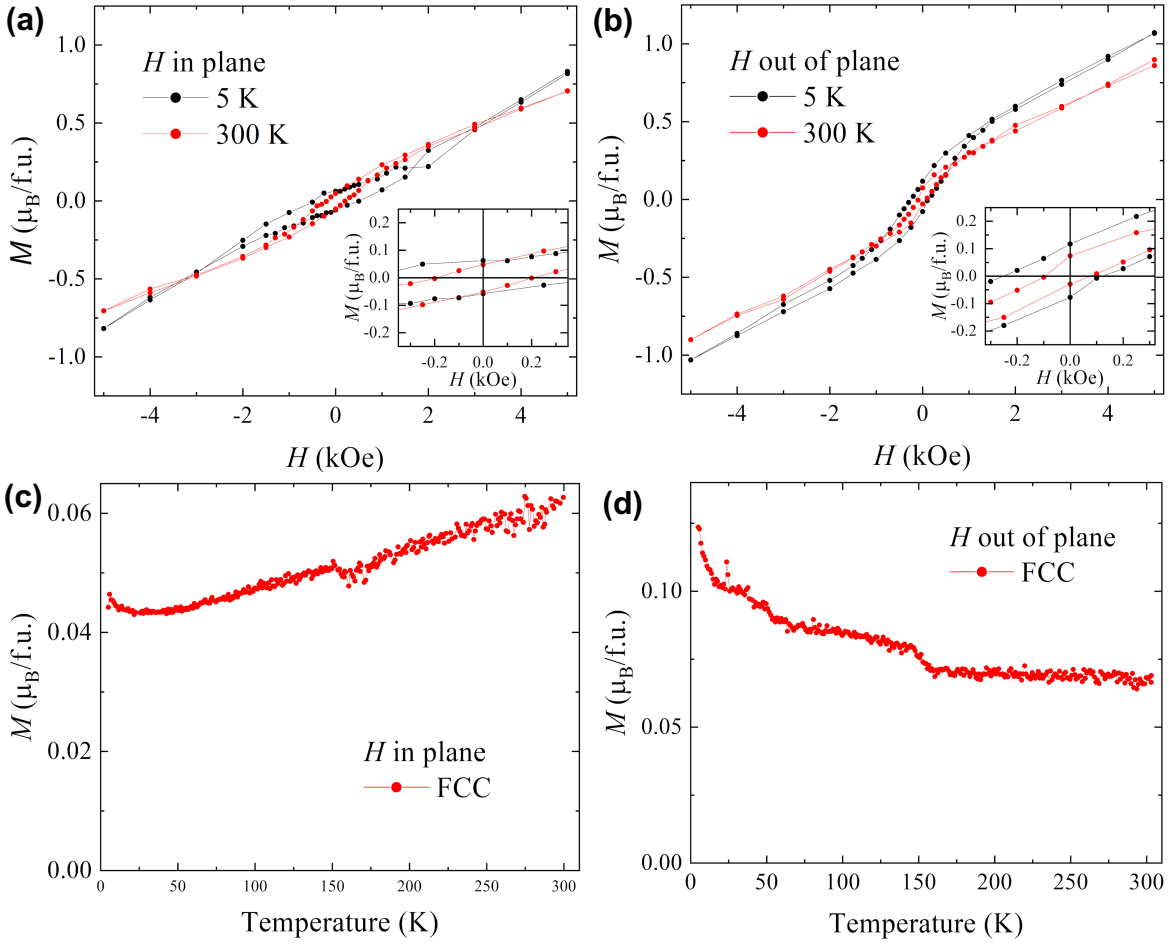

Fig. S16 Magnetisation *vs* applied field plots at 5 K and 300 K with a magnetic field applied in plane **(a)** and out of plane **(b)** of the deposited film. Magnetisation *vs* temperature data collected in a magnetic field of 250 Oe with the field applied either parallel **(c)** or perpendicular to the plane **(d)** of the deposited film for photoelectrodepositions using $MoCl_3$ - $CoCl_2$ electrolytes.

9 References

(1) P. A. Spevack and N. S. McIntyre, *J. Phys. Chem.*, 1992, 96, 9029-9035.

(2) M. C. Biesinger, B. P. Payne, A. P. Grosvenor, L. W. M. Lau, A. R. Gerson and R. St. C. Smart, *Appl. Surf. Sci.*, 2011, 257, 2717-2730.

(3) V. V. Romanov, V. A. Kozhevnikov, V. A. Mashkov and N. T. Bagraev, *Semiconductors*, 2020, 54, 1593-1597.